Computer Physics Communications 181 (2010) 1850–1858

Contents lists available at ScienceDirect

Computer Physics Communications

www.elsevier.com/locate/cpc

Seismic scalar wave equation with variable coefficients modeling by a new convolutional differentiator

Xiaofan Li *, Tong Zhu, Meigen Zhang, Guihua Long

Key Laboratory of the Earth's Deep Interior, CAS, Institute of Geology and Geophysics, Chinese Academy of Sciences, Beijing 100029, PR China

ARTICLE INFO

Article history:
Received 15 March 2010
Received in revised form 29 June 2010
Accepted 6 July 2010
Available online 13 July 2010

Keywords:
Wave equation with variable coefficients
Heterogeneous media
Accurate modeling of seismic wave
Localized operator
Suppression of numerical dispersion

ABSTRACT

Studying seismic wavefields in the Earth's interior requires an accurate calculation of wave propagation using accurate and efficient numerical techniques. In this paper, we present an alternative method for accurately and efficiently modeling seismic wavefields using a convolutional generalized orthogonal polynomial differentiator. Our approach uses optimization and truncation to form a localized operator. This preserves the fine structure of the wavefield in complex media and avoids non-causal interaction when parameter discontinuities are present in the medium. We demonstrate this approach for scalar wavefield modeling in heterogeneous media and conclude that the method could be readily extended to elastic wavefield calculations. Our numerical results indicate that this method can suppress numerical dispersion and allow for the study of wavefields in heterogeneous structures. The results hold promise not only for future seismic studies, but also for any field that requires high-precision numerical solution of partial differential equation with variable coefficients.

1. Introduction

Seismic waves are a powerful tool when exploring the Earth's interior. Such problems often involve multiple-scale heterogeneous structures, hence accurate and efficient methods for computing seismic wavefields are required when dealing with seismic wave propagation, seismic wave inversion, or high-resolution seismic wave imaging. However, it is difficult to obtain such accurate and efficient methods for computing or simulating seismic wavefields in highly heterogeneous media because this problem involves solving partial differential equations (wave equations) with variable coefficients. In general, numerical schemes for solving wave equations include direct methods and intermediate methods. In this paper, only numerical schemes for direct methods to treat the above-mentioned problem will be involved.

Several direct methods have been previously proposed for modeling seismic wavefields. These include the higher-order finite difference method [1,2], the finite element method [3], the spectral element method [4,5], the staggered grid Fourier pseudospectral method [6–8], the optimized FD method [9–12] and the convolutional differentiator method [13–17]. Each of these methods has its merits and drawbacks. For example, the finite element and spectral element methods have high calculation accuracy but are not very efficient and require substantial computational resources. The conventional higher-order finite difference method (HOFD) on regular grids is more efficient but suffers from poor numerical precision, especially in the high-frequency domain. Also, it is difficult to suppress numerical dispersion using the conventional HOFD approach [18]. The Fourier pseudospectral method is accurate and efficient for smooth functions (e.g., problems associated with smooth heterogeneous media), but a global operator is used when taking the Fourier transform which can lead to non-local interactions between globally-distant points. This is inconsistent with physical phenomena where interactions occur through local wave motion.

Finite difference (FD) methods could yield improved local accuracy with appropriate modification. For instance, optimally accurate second-order time-domain finite difference operators for modeling seismic waves [10,11] yield almost two orders of magnitude greater accuracy than the conventional $O(\Delta z^2, \Delta t^2)$ FD operator, while requiring twice as much CPU time. To increase the local accuracy of finite differences, a halfway staggered grid finite difference method has been used [6,12,17,19]. This approach improves the calculation precision and the ability to suppress numerical dispersion, but the use of a staggered grid requires additional computational overhead since derivatives must now be interpolated at the actual grid positions. The interpolation can be circumvented, as suggested by [9], by designing a grid system that compensates for the shifting property of the differentiator.

Although the convolutional differentiator method is equivalent to the finite difference method in substance, the tapered differentiator does have some distinct advantages over both the high-order finite difference method and the Fourier method. The convolutional differentiator method can simulate both local and global wavefield regimes in strongly heterogeneous media. It is also as efficient as

* Corresponding author.
E-mail address: xflee@mail.iggcas.ac.cn (X. Li).

0010-4655/$ – see front matter
doi:10.1016/j.cpc.2010.07.009

both the Fourier pseudospectral method and the low-order finite difference method, and uses a shorter operator (e.g., a five-point or nine-point operator). Holberg [9] investigated the design of convolutional operators for spatial differentiation in wave equation computations, with an emphasis on limiting the computational effort. Mora [13] applied convolutional differentiators for derivatives to elastic wave modeling, however, he did not give explicit expressions for the differentiators. Etgen [14] used the same method and explored wave propagation simulations in general anisotropic media.

Recently, an optimal and nearly analytic discrete method (ONADM) has also been developed [20,21]. Although the method has high calculation precision, its calculation efficiency still requires improvement and we do not discuss the method further.

In this paper, we present an alternative method for accurately and efficiently modeling seismic wavefields using a convolutional generalized orthogonal polynomial differentiator (CGOPD). To improve the calculation accuracy of the convolutional differentiator method and avoid Gibbs and Runge phenomena, we substitute the generalized orthogonal polynomial differentiator for the conventional high-order FD differentiator and introduce a Gaussian window function into the convolutional differentiator. Theoretically, the CGOPD (a short operator) is a localized operator that can describe both the fine structure of wavefields in complex media and avoid any non-causal interaction of the propagating wavefields when parameter discontinuities are present in the medium. The operator is truncated for practical implementation. Nine-point operators (optimized eighth-order operators) on regular grids are used as a compromise between computational efficiency and accuracy. Moreover, the CGOPD approach is computationally simpler and more efficient than implicit convolutional differentiator approaches [13,14] because it is explicit. As an example, we apply the convolutional differentiator to seismic scalar wavefield modeling in heterogeneous media. Our numerical results indicate that the CGOPD is suitable for large-scale numerical modeling since it effectively suppresses numerical dispersion by discretizing the wave equation when coarse grids are used.

2. Basic theory and method

2.1. The convolutional differentiator expression of the scalar seismic wave equation

Generally, the scalar wave equation with variable coefficients for 2D arbitrarily heterogeneous media in the time domain can be written as

$$\frac{1}{v^2}\frac{\partial^2 u(x,y,t)}{\partial t^2} = \frac{\partial^2 u(x,y,t)}{\partial x^2} + \frac{\partial^2 u(x,y,t)}{\partial y^2} + f(x,y,t), \tag{1}$$

where u is the scalar wavefield, v is the velocity of the wave, f is the body force, x and y are Cartesian coordinates, and t is the time. In the convolutional differentiator method, the spatial derivatives of u in Eq. (1) can be written as

$$\frac{\partial^2 u(x,y,t)}{\partial x^2} = d_1(x) * \big[d_1(x) * u(x,y,t)\big], \tag{2}$$

where '$*$' stands for convolution with respect to x and $d_1(x)$ is the convolutional differentiator for the first-order derivative. Similarly, $d_2(x)$ is the convolutional differentiator for the second-order derivative. Therefore, Eq. (1) can be expressed as

$$\frac{\partial^2 u(x,y,t)}{\partial t^2} = v^2(x,y,t)\big\{d_2(x) * u(x,y,t) + d_2(y) * u(x,y,t)\big\} + f(x,y,t), \tag{3}$$

where $d_2(x) = d_1(x) * d_1(x)$.

2.2. The convolutional generalized orthogonal polynomial differentiator

We first present the generalized orthogonal polynomial differentiator. The generalized orthogonal interpolation polynomial [22] can be written as

$$\varphi(x) = C_0 P_0(x) + \sum_{j=1}^{n} C_j P_j(x), \tag{4}$$

where the following values and recursion relationships apply:

$$\begin{aligned}
&P_0 = 1,\\
&P_1(x) = (x-\alpha_1)P_0(x),\\
&P_2(x) = (x-\alpha_2)P_1(x) - \beta_1 P_0(x),\\
&P_3(x) = (x-\alpha_3)P_2(x) - \beta_2 P_1(x),\\
&\quad\vdots\\
&P_{j+1}(x) = (x-\alpha_{j+1})P_j(x) - \beta_j P_{j-1}(x),\\
&\alpha_1 = \frac{1}{m}\sum_{i=1}^{m} x_i, \qquad \alpha_{j+1} = \frac{\sum_{i=1}^{m} x_i P_j^2(x_i)}{\sum_{i=1}^{m} P_j^2(x_i)},\\
&\beta_j = \frac{\sum_{i=1}^{m} x_i P_j(x_i) P_{j-1}(x_i)}{\sum_{i=1}^{m} P_{j-1}^2(x_i)},\\
&C_0 = \frac{\sum_{i=1}^{m} f(x_i) P_0(x_i)}{\sum_{i=1}^{m} P_0^2(x_i)}, \qquad C_j = \frac{\sum_{i=1}^{m} f(x_i) P_j(x_i)}{\sum_{i=1}^{m} P_j^2(x_i)}.
\end{aligned}$$

In these expressions, m is the number of data points, n is the order of the generalized orthogonal polynomial, and $f(x_i)$ is the value of the function $f(x)$ at point x_i. The $P_0(x), \ldots, P_{j+1}(x)$ are the system of generalized orthogonal polynomials used to construct the convolutional differentiator.

From Eq. (4), the generalized orthogonal polynomial derivative formula can be easily constructed as

$$\varphi'(x) = \frac{d\varphi(x)}{dx} = C_1 + \sum_{j=2}^{n} C_j P_j'(x), \tag{5}$$

where

$$\begin{aligned}
&P_j'(x) = \frac{dP_j(x)}{dx}, \quad \text{and}\\
&P_1'(x) = P_0(x),\\
&P_2'(x) = P_1(x) + (x-\alpha_2)P_1'(x),\\
&P_3'(x) = P_2(x) + (x-\alpha_3)P_2'(x) - \beta_2 P_1'(x),\\
&\quad\vdots\\
&P_{j+1}'(x) = P_j(x) + (x-\alpha_{j+1})P_j'(x) - \beta_j P_{j-1}'(x).
\end{aligned}$$

The generalized orthogonal polynomial differentiator is then written as

$$\frac{d}{dx} = C_1^d + \sum_{j=2}^{n} C_j^d P_j'(x), \tag{6}$$

where

$$C_j^d = \frac{\sum_{i=1}^{m} P_j(x_i)}{\sum_{i=1}^{m} P_j^2(x_i)}.$$

Similarly, the convolutional differentiator for the second-order derivative can be written as

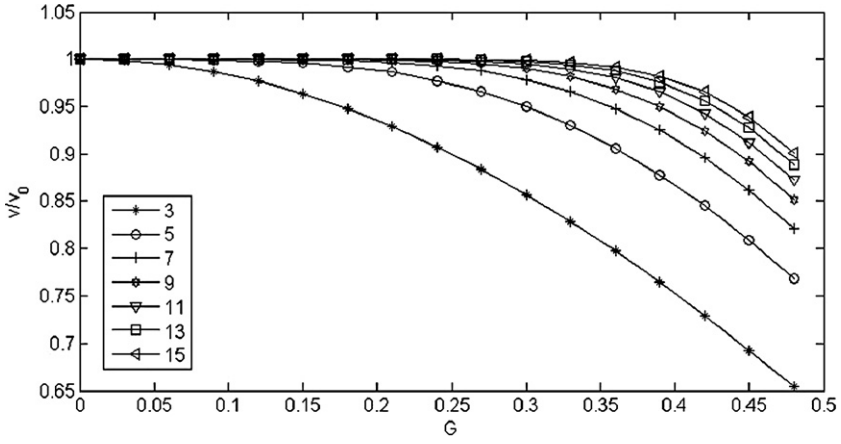

Fig. 1. The dispersion relation for the CGOPD approach for the one-dimensional homogeneous wave equation. V_0 is the acoustic velocity, V is the phase velocity, G is the inverse of the number of grids per highest wavelength ($k\Delta x/2\pi$, where $k = \omega/V_0$), and the numbers in the label frame stand for the length of the operator.

$$\frac{d^2}{dx^2} = \sum_{j=2}^{n} C_j^d P_j''(x), \tag{7}$$

where

$$\begin{aligned}
&P_1''(x) = \frac{d^2 P_1(x)}{dx^2} = 0,\\
&P_2''(x) = 2P_1''(x),\\
&P_3''(x) = 2P_2''(x) + 2(x - \alpha_3),\\
&\quad\vdots\\
&P_{j+1}''(x) = 2P_j'(x) + (x - \alpha_{j+1})P_j''(x) - \beta_j P_{j-1}'''(x).
\end{aligned}$$

To discretize the differentiator, we let $x = i\Delta x$. In the discrete domain, Eqs. (6) and (7) can then be written as

$$d_1(i\Delta x) = C_1^d + \sum_{j=2}^{n} C_j^d P_j'(i\Delta x) \tag{8}$$

and

$$d_2(i\Delta x) = \sum_{j=2}^{n} C_j^d P_j''(i\Delta x). \tag{9}$$

Here i is the sampling index and Δx is the sampling rate along the x axis. For practical implementation, the differentiator has to be truncated as a short operator, but doing so could lead to the Gibbs phenomenon. On the other hand, the Runge phenomenon caused by polynomial interpolation is very obvious. To avoid these phenomena, we use a Gaussian window function for truncating the differentiator:

$$w(n) = ce^{-an\Delta x^2}, \quad |n| = 0, 1, 2, \ldots, mx, \tag{10}$$

where mx is the one-side truncation length in sampling number, c is a constant, and a ($0.1 \leqslant a \leqslant 0.75$) is an attenuation factor. For wave equation modeling, the attenuation factor a is dependent on the dominant frequency of wavefield. Generally, $a \propto 2\pi f_0/v$ where f_0 is the dominant frequency of wavefield, v is the wave velocity. A modified and practical convolutional differentiator can be denoted by

$$\begin{aligned}
&\hat{d}_1(i\Delta x) = \begin{cases} (-1)^i d_1(i\Delta x)w(i), & i = 1, 2, \ldots, m,\\ -\hat{d}_1(j\Delta x), & i = 1, -2, \ldots, -m,\ j = -i, \end{cases}\\
&\hat{d}_1(0\Delta x) = 0.
\end{aligned} \tag{11}$$

For the second-order derivative, the convolutional differentiator is written as $\hat{d}_2(i\Delta x)$.

2.3. The discrete seismic modeling formula and its stability condition and accuracy

For seismic modeling in the discrete domain, the solution of seismic scalar wave equation (3) can be written as

$$\begin{aligned}
u(m, n, t + \Delta t) &= 2u(m, n, t) - u(m, n, t - \Delta t)\\
&\quad + v^2(m, n)\Delta t^2 \Bigg[\Delta x \sum_{i=-mx}^{mx} \hat{d}_2(i\Delta x)u(m - i, n, t)\\
&\quad + \Delta z \sum_{j=-nz}^{nz} \hat{d}_2(j\Delta z)u(m, n - j, t) + f(m, n, t) \Bigg],
\end{aligned} \tag{12}$$

where m and n are indices along the discrete x and z axes, Δx, Δz and Δt are sampling rates along the x, z and t axes, mx and nz are the half differentiator lengths in sampling number along the x and z axes, and $\hat{d}_2(i\Delta x)$ is the CGOPD operator. Here we apply the second-order central finite difference method to the temporal derivative. Note that in Eq. (12), the spatial derivative operator is not based on a Taylor expansion.

It can be shown that the stability criteria of equation (12) for 2D homogeneous media is similar to that of the perfect Fourier derivate [23], namely

$$\Delta t \leqslant \frac{\min(\Delta x, \Delta z)}{v}. \tag{13}$$

Similarly, for 2D heterogeneous media, the stability condition can be written as

$$\Delta t \leqslant \frac{\min(\Delta x, \Delta z)}{v_{\max}}(1 + \varepsilon), \tag{14}$$

where $v_{\max}$ is the maximum velocity of the medium and ε is a finite but relatively small number whose amplitude and sign depend on the nature of the question.

Previous works generally evaluated the proposed computational schemes by presenting theoretical derivations or by conducting numerical tests for a homogeneous medium, using the numerical dispersion of the phase velocity as the criterion for evaluating accuracy. This approach is demonstrated in Fig. 1, which plots the dispersion relation for the CGOPD method for the 1D homogeneous wave equation. The error analysis is only for the first derivative operators. In this plot, V_0 is the acoustic velocity, V is the phase velocity, G is the inverse of the number of grids per highest wavelength ($k\Delta x/2\pi$, where $k = \omega/V_0$), and the numbers in the label frame of Fig. 1 denote the length of the operator. The plot of

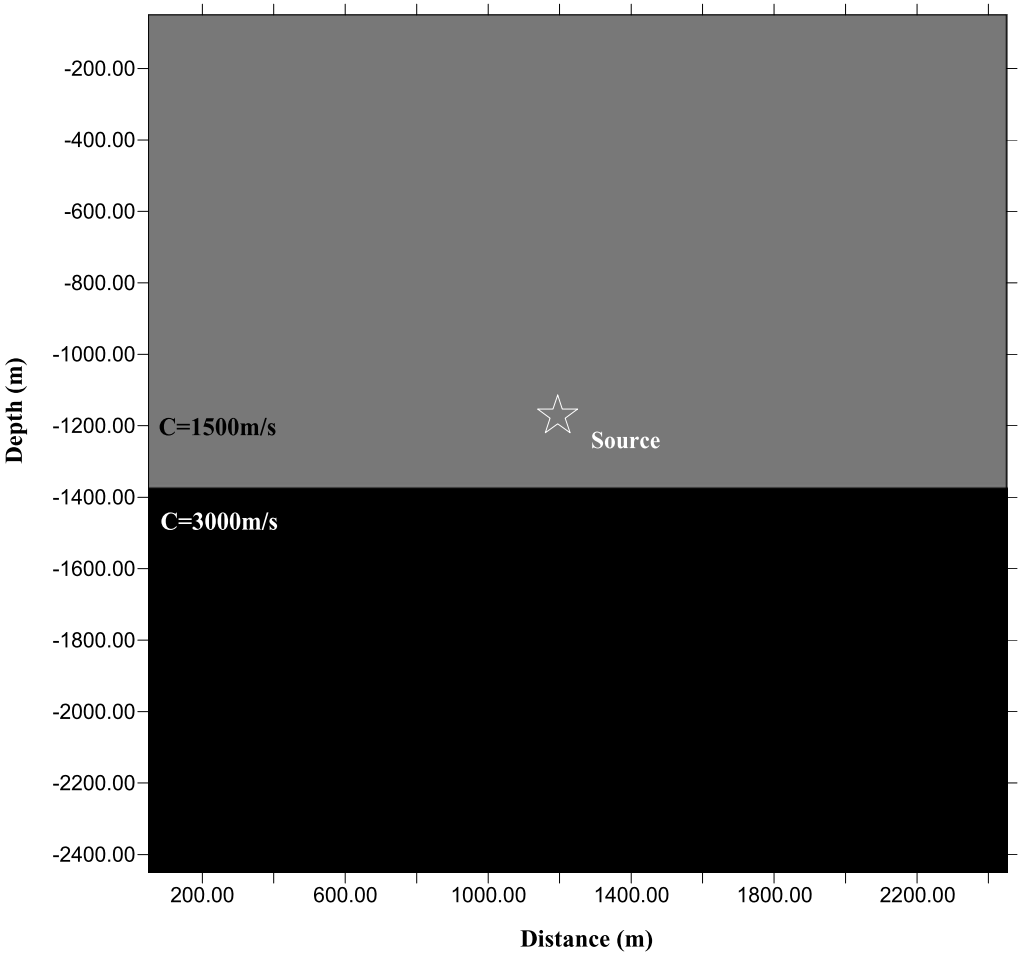

Fig. 2. Two-layered medium model; configuration and parameters.

the dispersion relation may be considered as the reference criterion for designing the convolutional differentiator. From these curves, it can be seen that the accuracy of the operator clearly depends on its length. After comparing detailed synthetic testing, the nine-point differentiator performs adequately. However, seismologists typically focus on wave propagation in heterogeneous models that approximate the actual Earth, which is highly heterogeneous. Therefore, we will evaluate the accuracy and performance of Eq. (12) for the case of heterogeneous models in the next section.

3. Numerical examples

Generally, the accuracy of numerical schemes is evaluated by considering the numerical dispersion as a function of number of grid points per wavelength. Even though the wavefield in a highly heterogeneous medium is usually not known analytically, the overall performance of the algorithm can still be judged through numerical results qualitatively. In this section, we give two numerical examples for evaluating the performance of the CGOPD approach. It is well known that the conventional FD method is one of the most efficient numerical schemes for partial differential equation with variable coefficients. The CGOPD approach and the conventional FD method are equivalent in the computational efficiency because the CGOPD approach is an optimized FD method in nature. Therefore, we compare the CGOPD approach and the conventional FD method only in the computational accuracy in this section.

3.1. Seismic scalar wavefield in a two-layered medium with high velocity contrast

Like other optimized high-order FD schemes, the CGOPD is not based on a Taylor expansion. Aiming for a balance between efficiency and accuracy, we chose nine-point explicit operators (eighth-order operators) on regular grids. One might expect these operators to have a slightly reduced accuracy but still be faster than other operators (with an accuracy of approximately 3 grids per highest wavelength). Ultimately, if the CGOPD approach has only a slight advantage in accuracy compared to conventional high-order HOFD (the FD scheme based on Taylor expansions), then it is meaningless to adopt it.

We compared the numerical results found using CGOPD with those from conventional high-order FD for a two-layered medium with a high velocity contrast. The model consists of two different wave velocity regions separated by a horizontal interface (Fig. 2). The model parameters were a velocity of $C_1 = 1500$ m/s for the upper layer with the source, and a velocity of $C_2 = 3000$ m/s for the lower layer. The number of grid points was 241×241, the model size was 2400 m $\times$ 2400 m, and the wave source was located at $(x_s, z_s) = (1200\text{ m}, 1200\text{ m})$. The spatial increments were 10 m and the time increment was 1 ms. The interface can be considered a velocity discontinuity since the velocity contrast is very high. The source, a band-limited Ricker wavelet, is located in the upper layer and has an amplitude spectrum peak at 30 Hz and a high-frequency cut at 43 Hz.

Figs. 3A, 4B and 4C are wavefield snapshots at time marks of 200 ms, 300 ms and 400 ms generated by the CGOPD. The snap-

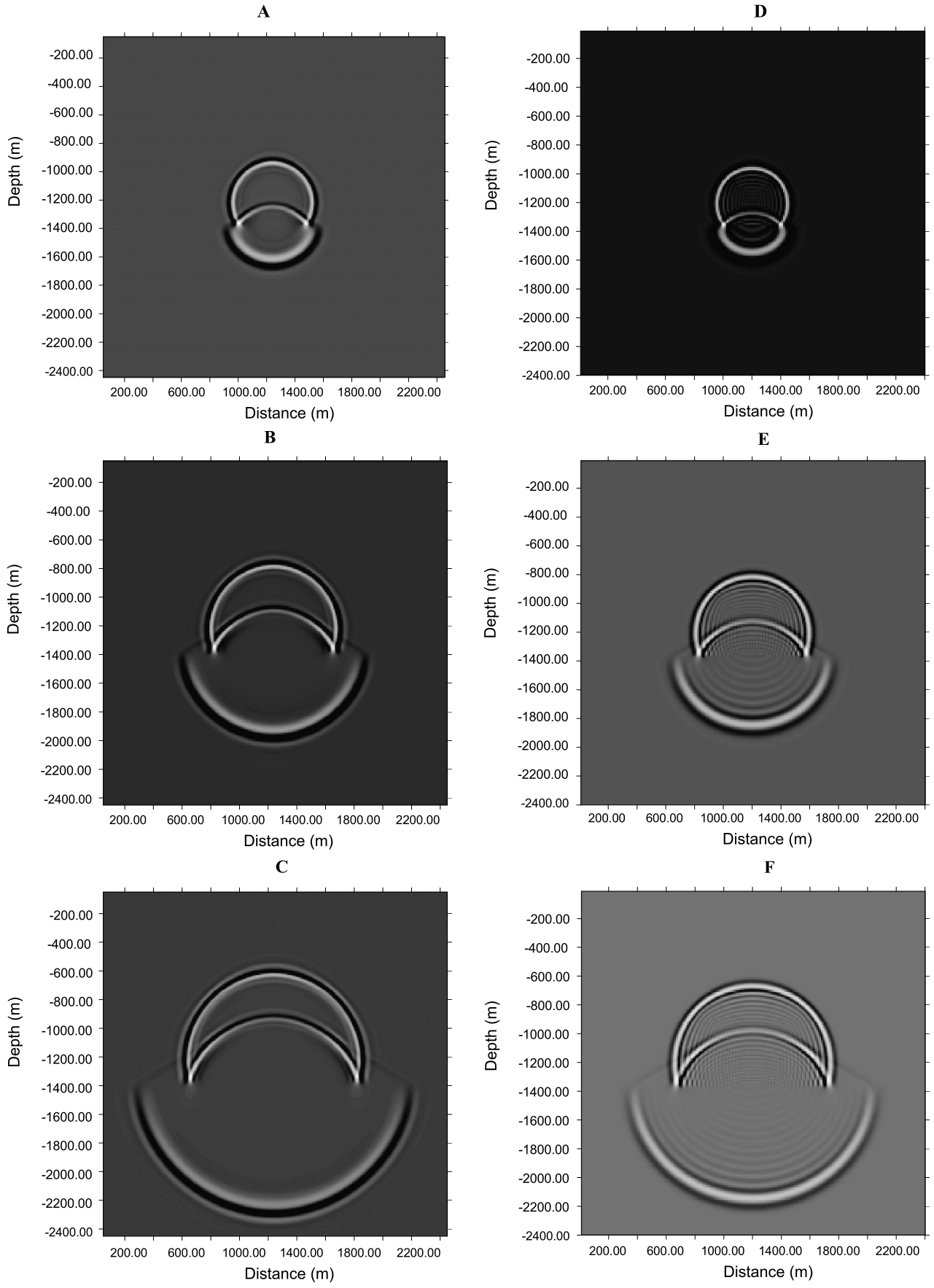

Fig. 3. Snapshots of seismic wavefields in a two-layered medium model generated by CGOPD at times (A) 200 ms, (B) 300 ms and (C) 400 ms. Snapshots of seismic wavefields in the same medium model generated by the eighth-order FD method at times (D) 200 ms, (E) 300 ms and (F) 400 ms.

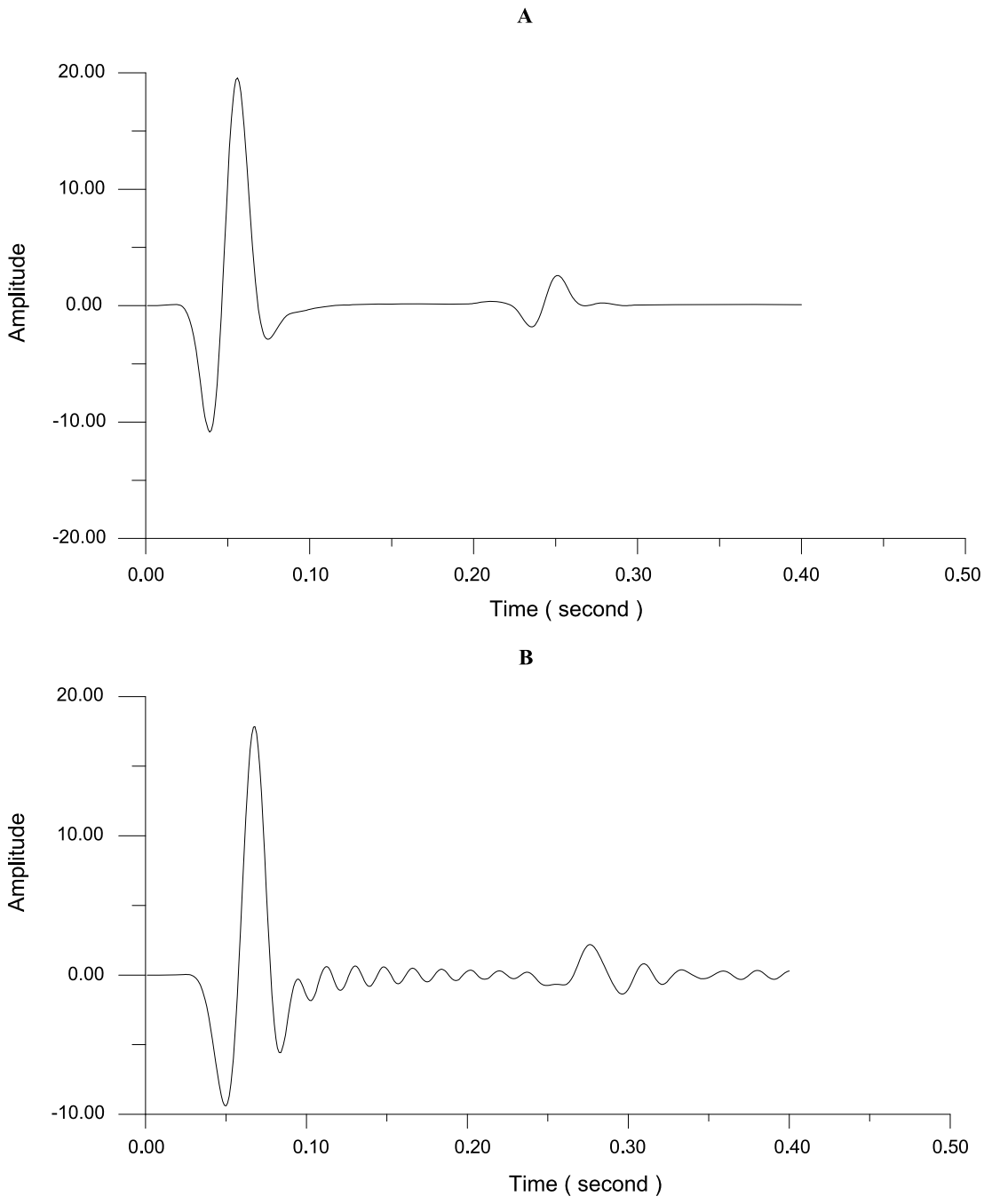

Fig. 4. Comparison of synthetic seismograms for a two-layered medium model generated by the CGOPD (A) and eighth-order FD (B).

shots in Figs. 3A, 3B and 3C clearly show that the wavefront of the direct wave exhibits a semi-circular shape at the inner interface. Other phases (e.g., the reflected and transmitted waves) are also displayed clearly. The wavefronts are continuous and mend the velocity discontinuity in the model. From these snapshots, it can be seen that the wavefields simulated by CGOPD are very clear. There is hardly any grid dispersion despite the fact that there are only 3.5 grids or less per shortest wavelength at the high-cut frequency.

Comparing wavefield snapshots generated by the CGOPD (Figs. 3A, 3B and 3C) with the eighth-order FD (Figs. 3D, 3E and 3F, respectively), one can see that there is hardly any evidence of numerical dispersion in the CGOPD approach, whereas numerical dispersion is obviously present when using the eighth-order FD method. A similar phenomenon also appears when comparing the synthetic seismograms (Fig. 4A for the CGOPD and Fig. 4B for the eighth-order FD). Note that the number of grid points (or sampling interval) is consistent between the two methods. Although the accuracy of the conventional HOFD can be improved by heavy over-sampling along the spatial axes, more computational resources would naturally be required. Therefore, the CGOPD is suitable for large-scale numerical modeling with coarse spatial grids.

Based on these results, we conclude that the convolutional operator designed here is accurate to about 3.5 grids or less per shortest wavelength. Also, the CGOPD method effectively captures the inner interface without any special treatment at the discontinuity.

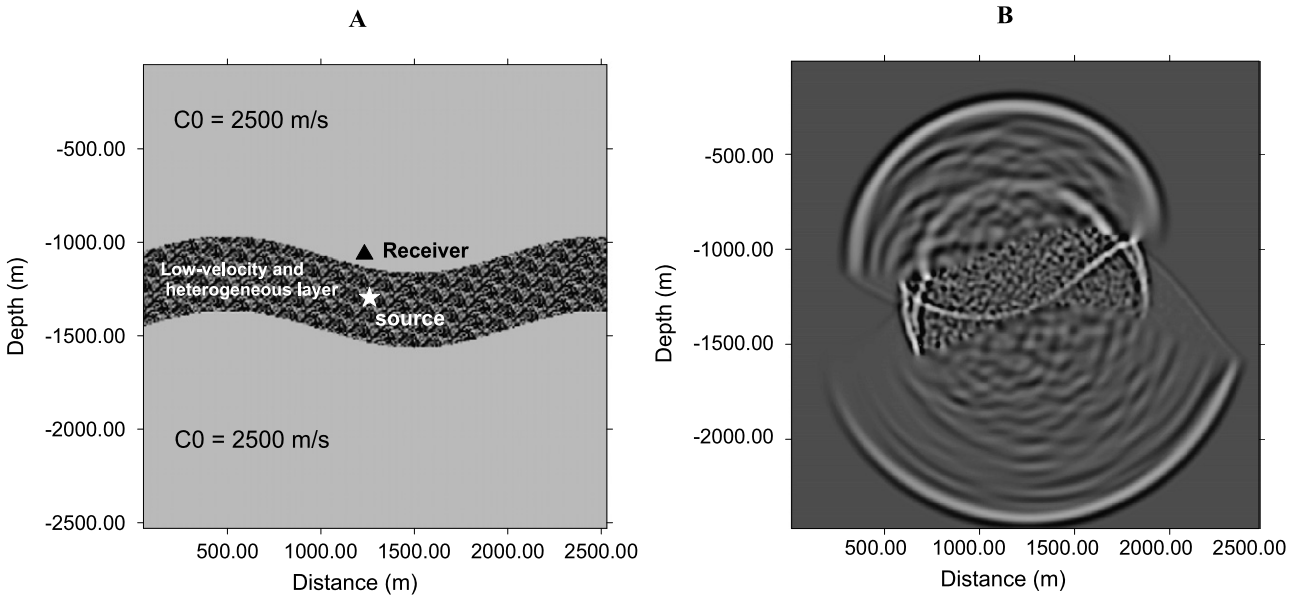

Fig. 5. Snapshot of seismic wavefields in a heterogeneous medium model generated by CGOPD. (A) Heterogeneous medium model; configuration and parameters. (B) Snapshot of the wavefield generated by CGOPD at time 450 ms.

3.2. Seismic scalar wavefield in a strongly heterogeneous medium

We next consider the more complex case consisting of a low-velocity and strongly heterogeneous layer embedded in a homogeneous host medium. The low-velocity layer has an average thickness of 500 m, a mean velocity of $C_1 = 1500$ m/s, and a velocity perturbation generated by random numbers with a uniform distribution between $\pm 30\%$. The velocity perturbation scale length is taken to be the grid spacing (10 m). The host layer has a velocity of $c = 3000$ m/s. The model is shown in Fig. 5A. The upper and lower surfaces of the heterogeneous zone are curved interfaces, and a seismic source simulated by a band-limited Ricker wavelet in the embedded zone is located at $(x_s, z_s) = (1235\text{ m}, 1235\text{ m})$. The source amplitude spectrum peaks at 30 Hz and the high-cut frequency is 43 Hz. The model is defined on a 2470 m $\times$ 2470 m grid with a grid spacing of 10 m in both spatial directions. Note that this model is defined by the strong contrast of velocities between the two zones.

Fig. 5B shows a snapshot of the full wavefield at 450 ms. Note that the seismic scalar waves from the interface, the curved interfaces, and some details of the low-velocity and heterogeneously curved zone are all clearly displayed. The snapshot also contains the direct, reflected, transmitted, and scattered waves. Fig. 6A presents the synthetic seismogram generated by the CGOPD in the previous medium model, clearly displaying the seismic coda from scattering. These results for a highly heterogeneous model have negligible numerical dispersion, which are accurate to approximately 3.5 grids or less per shortest wavelength in space. Fig. 6B shows the synthetic seismogram generated by the eighth-order FD method in the same medium model, which has obvious numerical dispersion (i.e. periodic oscillation waveforms after the head wave). The CGOPD, therefore, can readily cope with the question of seismic scattering and can simulate seismic waves in complicated geometries and highly heterogeneous media without any additional treatment.

In terms of efficiency, the computational speed of the CGOPD is very fast since the spatial derivative is a short explicit operator. For the model considered above, modeling the wavefield for 450 time steps only takes 60 seconds of CPU time running on a Core 2 Duo 2.5 GHz machine.

4. Conclusions

We have designed a convolutional differentiator using generalized orthogonal polynomials that is explicit and computationally simple and efficient. To obtain an optimal balance between computational efficiency and accuracy of the CGOPD approach, we chose nine-point explicit operators (optimized eighth-order operators) on regular grids. It is easier to implement the CGOPD scheme since the corresponding operator is explicit. The nine-point CGOPD is a localized operator that can describe the local properties of complicated wavefields and avoid non-causal interaction of the propagating wavefield when parameter discontinuities are present in the medium. This approach is therefore suitable for large-scale numerical modeling since it effectively suppresses numerical dispersion by discretizing the wave equations when coarse grids are used.

In methodology, the conventional FD scheme is based on Taylor expansions. In nature, the CGOPD approach is an optimized FD method in which the spatial derivative operator is not based on a Taylor expansion. The CGOPD operator can easily be designed by the generalized orthogonal polynomial, truncating to the desired length, and multiplying by the Gaussian window to avoid Gibbs and Runge phenomena. It is simpler than the Taylor expansion approach which requires some tedious algebra. From the numerical results (Figs. 3, 4 and 6), it can be seen that the CGOPD scheme is superior to the conventional FD scheme in suppression of numerical dispersion. Moreover, the CGOPD approach is computationally simpler and more efficient than implicit convolutional differentiator approaches [13,14] because it is explicit.

From the simulation results in this paper, it has been shown that the CGOPD method can effectively capture the inner interface without any special treatment at the discontinuity; therefore, it can simulate seismic waves in complicated geometries and highly heterogeneous media without any additional treatment. The CGOPD allows us to use a coarse grid, that is, fewer samples per wavelength, to achieve the same accuracy in modeling waves and is similar to that obtained by conventional FD schemes on a finely-sampled grid. The results here hold promise not only for future geophysical studies, but also for any field that requires high-precision numerical solution of partial differential equation with variable coefficients. Although the CGOPD method is only applied to the 2D scalar wavefield calculation for highly heterogeneous

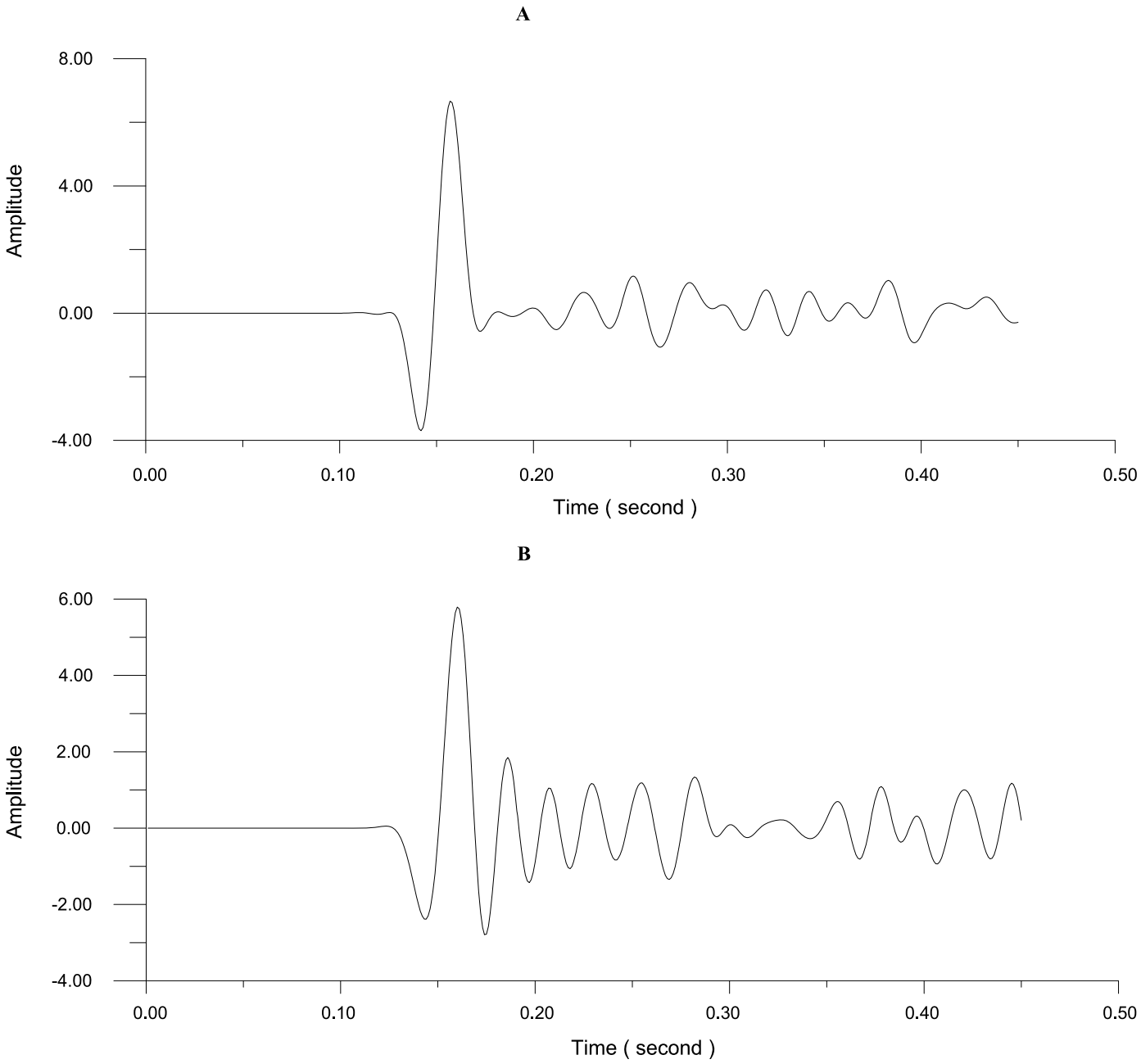

Fig. 6. Synthetic seismograms for a heterogeneous medium model of Fig. 5A, generated by CGOPD (A) and eighth-order FD (B).

models in this paper, the method can be easily extended to 3D elastic wavefield calculations. For 3D elastic wavefield calculations, the computational efficiency and accuracy will be analyzed in a later paper.

Acknowledgements

This work has been supported by the National Natural Science Foundation of China (Grant No. 40437018, 40874024) and the Ministry of Science and Technology of People's Republic of China (973 Project, Grant No. 2007CB209603).

References

[1] A. Bayliss, K.E. Jordan, B.J. LeMesurier, E. Turkel, A fourth-order accurate finite-difference scheme for the computation of elastic waves, Bull. Seism. Soc. Am. 76 (1986) 1115–1132.
[2] A.R. Levander, Fourth-order finite-difference P–SV seismograms, Geophysics 53 (1988) 1425–1435.
[3] Z.J. Zhang, G.J. Wang, J.M. Harris, Multi-component wave-field simulation in viscous extensively dilatancy anisotropic media, Phys. Earth Planet. Interiors 114 (1999) 25–38.
[4] D. Komatitsch, J.P. Vilotte, The spectral element method: an efficient tool to simulate the seismic response of 2D and 3D geological structures, Bull. Seism. Soc. Am. 88 (1998) 368–392.
[5] D. Komatitsch, J. Tromp, Spectral-element simulation of global seismic wave propagation—I. Validation, Geophys. J. Int. 149 (2002) 390–412.
[6] B. Fornberg, High order finite differences and pseudospectral method on staggered grids, SIAM J. Numer. Anal. 27 (1990) 904–918.
[7] H.W. Chen, Staggered grid pseudospectral simulation in viscoacoustic wavefield simulation, J. Acoust. Soc. Am. 100 (1996) 120–131.
[8] Z. Zhao, J. Xu, H. Shigeki, Staggered grid real value FFT differentiation operator and its application on wave propagation simulation in the heterogeneous medium, Chinese J. Geophys. 46 (2) (2003) 234–240 (in Chinese).
[9] O. Holberg, Computational aspects of the choice of operator and sampling interval for numerical differentiation in large-scale simulation of wave phenomena, Geophys. Prosp. 35 (1987) 629–655.

[10] R.J. Geller, N. Takeuchi, Optimally accurate second-order time-domain finite difference scheme for the elastic equation of motion: one-dimensional case, Geophys. J. I 135 (1998) 48–62.

[11] N. Takeuchi, R.J. Geller, Optimally accurate second-order time-domain finite difference scheme for computing synthetic seismograms in 2-D and 3-D media, Phys. Earth Planet. Interiors 119 (2000) 99–131.

[12] P. Moczo, J. Kristek, V. Vavrycuk, R.J. Archuleta, L. Halada, 3D heterogeneous staggered-grid finite-difference modeling of seismic motion with volume harmonic and arithmetic averaging of elastic moduli and densities, Bull. Seism. Soc. Am. 92 (2002) 3042–3066.

[13] P. Mora, Elastic finite-difference with convolutional operators, Stanford Exploration Project 48 (1986) 272–289.

[14] J.T. Etgen, Finite-difference elastic anisotropic wave propagation, Stanford Exploration Project 56 (1987) 23–57.

[15] D. Kosloff, D. Kessler, Seismic numerical modeling, in: Y. Desaubies, A. Tarantla, J. Zinn-Justin (Eds.), Oceanographic and Geophysical Tomography, Elsevier Sci. Publ., Amsterdam, 1990, pp. 249–312.

[16] B. Zhou, S.A. Greenhalgh, Seismic scalar wave equation modeling by a convolutional differentiator, Bull. Seism. Soc. Am. 82 (1982) 289–303.

[17] K. Yomogida, J.T. Etgen, 3-D wave propagation in the Los Angeles Basin for the Whittier–Narrows earthquake, Bull. Seism. Soc. Am. 83 (1993) 1325–1344.

[18] S.Q. Wang, D.H. Yang, K.D. Yang, Compact finite difference scheme for elastic equations, J. Tsinghua Univ. (Sci. & Tech.) 42 (2002) 1128–1131.

[19] A. Pitarka, 3D elastic finite-difference modeling of seismic motion using staggered grids with nonuniform spacing, Bull. Seism. Soc. Am. 89 (1999) 54–68.

[20] D.H. Yang, J.M. Peng, M. Lu, An nearly-analytic discrete method for wavefieldsimulation in 2D porous media, Commun. Comput. Phys. 1 (2006) 528–547.

[21] D.H. Yang, G.J. Song, M. Lu, Optimally accurate nearly analytic discrete scheme for wave-field simulation in 3D anisotropic media, Bull. Seism. Soc. Am. 97 (2007) 1557–1569.

[22] J. Xie, Mathematical Method for Geophysical Data Process, Geological Publishing House, Beijing, 1981, pp. 97–104 (in Chinese).

[23] D. Kosloff, M. Reshef, D. Loewenthal, Elastic wave calculations by Fourier mathod, Bull. Seism. Soc. Am. 74 (1984) 875–891.